Runaway electron transport via tokamak microturbulence

T. Hauff and F. Jenko
Max-Planck-Institut für Plasmaphysik, EURATOM Association, 85748 Garching, Germany

(Received 6 July 2009; accepted 14 September 2009; published online 27 October 2009)

The mechanisms found for the magnetic transport of fast ions in the work of Hauff *et al.* [Phys. Rev. Lett. **102**, 075004 (2009)] are extended to the diffusion of runaway electrons. Due to their smaller mass and larger energy, they behave strongly relativistically, for which reason the scaling laws defined previously have to be modified. It is found that due to these changes, the regime of constant magnetic transport does not exist anymore, but diffusivity scales with E^{-1} for magnetic transport, or even with E^{-2} in the case that finite gyroradius effects become important. It is shown that the modified analytical approaches are able to explain the surprisingly small values found in experiments, although it cannot be excluded that possibly other reduction mechanisms are present at the same time. © *2009 American Institute of Physics*. [doi:10.1063/1.3243494]

I. INTRODUCTORY REMARKS

The anomalous transport of particles, momentum, and energy in magnetically confined plasmas is known to be induced by electrostatic and magnetic fluctuations. In this context, the interaction of fast particles with the turbulent structures is of great interest for present as well as future fusion devices. In Ref. 1, we have studied the transport behavior of fast ions with energies up to the MeV range. They are created in fusion processes (alpha particles) or launched into the plasma by neutral beam injection (NBI). We applied the test particle approach since their density is small and their velocities and orbits are clearly distinct from the bulk plasma. In the present publication, we use the mechanisms introduced in Refs. 1 and 2 in order to describe the transport behavior of *runaway electrons*. In contrast to alpha particles or beam ions, they are created in the plasma by accident and can have a serious impact on the inner vessel wall. Although, in principle, their orbits are similar to the suprathermal ion orbits, important differences occur. For example, the transport is now dominated by magnetic fluctuations, and relativistic effects become dominant. Both effects are due to the much larger parallel velocities of the electrons.

In a tokamak, situations can occur where large electric fields are induced. This may happen during so-called *disruption* events, when the fast cooling of the plasma drastically reduces its conductivity ($\sigma \propto T_e^{3/2}$). According to Lenz's law, the sudden reduction in the toroidal current induces a large toroidal electric field. In that case, some electrons experience unlimited "runaway" acceleration. The reason for this behavior is that the friction force $F(v)$ acting on an electron is a nonmonotonic function of the particle's velocity having a global maximum around the thermal speed v_{th}. For electrons moving faster, the characteristic collision frequency can be derived as[3]

$$\nu_e = \frac{e^4 n_e \ln \Lambda}{4\pi\epsilon_0^2 m_e^2 v^3}, \tag{1}$$

where $\Lambda \equiv \lambda_D/\lambda_L$ is the ratio of the *Debye length* and the *Landau length* of the plasma. Thus, for a sufficiently fast electron in a sufficiently large field, the friction force gets smaller and smaller, and the particle accelerates until the electric field force is balanced by another mechanism, particularly the synchrotron radiation of the particle. The runaway electrons are accelerated to energies of several tens of MeV in existing tokamaks as TEXTOR[4–6] or JET (Ref. 7) or, as expected for ITER, up to 500 MeV in the worst case scenario.[8] If these fast particles hit the vessel wall, they can cause substantial damage. Although this constitutes a serious concern already in present-day tokamaks, it has been predicted that in ITER, not only the maximum energy of runaways but also their number will be increased due to the secondary generation caused by the avalanche mechanism. It is therefore obvious that the diffusion mechanisms of runaway electrons are of great interest. Since, as we have seen, runaway electrons are extremely collisionless, the application of the test particle model is justified to an exceptionally high degree.

Similar to the diffusion of fast ions described in previous publications,[1,2] we find that the basic mechanisms of transport seem to be not completely understood. Most works on this topic find that the experimentally measured transport is one or more orders of magnitude smaller than the theoretical prediction based on magnetic field line diffusion. According to that approach, the particles just follow the turbulent magnetic field lines. If we denote the mean perpendicular magnetic drift velocity for a particle just following the magnetic field lines by $V_B \sim \tilde{B}_r/B_0 v_\parallel$ (where $\tilde{B}_r$ is the root mean square of the perturbed radial magnetic field) and assume a parallel decorrelation at $\tau_\parallel = \lambda_\parallel/v_\parallel \sim \pi q R_0/v_\parallel$, we obtain, according to the ansatz $D = V^2\tau$ (small Kubo number limit)

$$D_M = \pi q R_0 \left(\frac{\tilde{B}_r}{B_0}\right)^2 v_\parallel \Upsilon \tag{2}$$

for the magnetic diffusion coefficient. Here, B_0 is the magnetic background field, $\tilde{B}_r$ is its radial perturbative part, τ is the effective decorrelation time of a particle, q is the safety factor, and R_0 is the major radius of the tokamak. Υ is a factor introduced in order to describe finite orbit size effects and is defined below in some variations. The introduction of

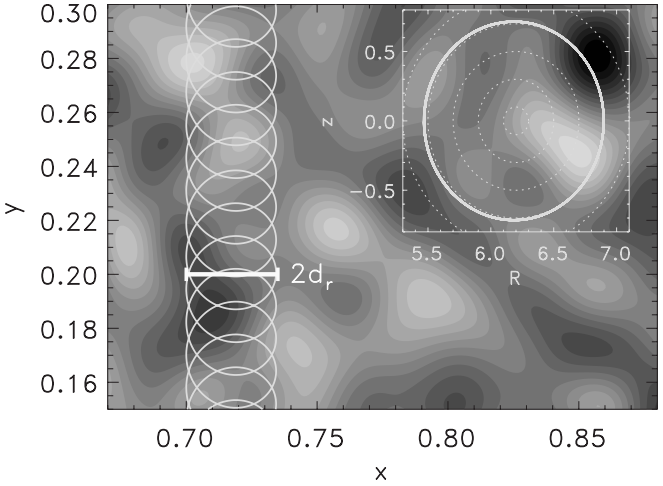

FIG. 1. Drift orbit of a passing particle (in a fluctuating potential) in field-aligned coordinates (left-hand side) and in cylindrical coordinates (embedded). Some magnetic flux surfaces are shown for comparison. The particle oscillates in the x (radial) direction with a radius of d_r, as well as in the y (toroidal) direction with a similar radius. In addition, there is a constant precession drift in the toroidal direction.

Υ is originally[9] based on a reduction in the magnetic drift velocity V_B but does not change the transition of the particle motion into the diffusive regime since it is still assumed that the particles follow—averaged—magnetic field lines, and that the decorrelation occurs by motion parallel to the magnetic field.

The electrostatic transport, in contrast, is denoted by

$$D_E = \pi q R_0 V_E^2 / v_\parallel \Upsilon, \tag{3}$$

where V_E is the mean $E \times B$ drift velocity. Equations (2) and (3) make clear why for runaway electrons only the magnetic transport is assumed to be relevant, in general. Now, experimental measurements in tokamaks such as JET,[7] TEXTOR-94,[4–6] or the Madison Symmetric Torus[10] have shown that the diffusion coefficient of the runaway electrons is one or more orders of magnitude smaller than that predicted by Eq. (2) (setting $\Upsilon = 1$). Experimental values are found to be, for example, $D \approx 0.2$ m^2/s at JET, $D \approx 0.01$ m^2/s at TEXTOR-94, and $D \approx 3$ m^2/s at the Madison Symmetric Torus.

Two possible explanations have been put forward in order to explain the rather low transport level. The first explanation (used, e.g., in Refs. 6, 7, 11, and 12) attributes the reduction to drift orbit averaging effects similar to what was done in the past for fast beam ions (see the discussion in Ref. 2). *Orbit averaging* means that the small deviations of a particle from its initial field line (see Fig. 1), which are caused by magnetic drifts, are treated by averaging the fluctuating component of the magnetic field over a certain structure, e.g., a circle as described below, hence reducing its influence. The standard reference that was used in these works is Ref. 9, where the effect of orbit averaging was included by multiplying Eq. (2) with a factor

$$\Upsilon \sim \lambda_B / d_r, \tag{4}$$

where λ_B is the correlation length of the magnetic field fluctuations and d_r is the drift orbit radius. This is equivalent (except for the prefactor) to the influence of gyroaveraging for large gyroradii and small Kubo numbers which was derived in Ref. 13, replacing ρ_g by d_r/λ_B, which finally leads to

$$\Upsilon' = [1 - 2(d_r/\lambda_B)^2 + 5/2(d_r/\lambda_B)^4 - \cdots]^2 \quad \forall \quad d_r/\lambda_B \lesssim 1,$$
$$\Upsilon' = \lambda_B/(4\sqrt{\pi} d_r) \quad \forall \quad d_r/\lambda_B \gtrsim 1. \tag{5}$$

This treatment of orbit averaging—which is based on a direct averaging of the streamfunction over a ring with radius d_r—gives a reduction factor that is almost one order of magnitude below the one given in Ref. 9 for $d_r/\lambda_B \gtrsim 1$. However, the problem remains that the validity of the orbit averaging approach has to be taken for granted. In the publications cited above, this topic is not discussed. Moreover, Eq. (2), together with the factor Υ, has been widely used to determine the perturbed magnetic field strength $\tilde{B}_r/B_0$ (Refs. 6 and 7) so that the validity of the approach could not be justified by directly comparing measurements of D and $\tilde{B}_r/B_0$. In Sec. II, a validity condition for the orbit averaging approach is given.

The second explanation for the transport reduction of runaway electrons that is used in literature is the assumption that in the torus the so-called "good surfaces" exist, where there is no stochasticity of magnetic field lines, and therefore the cross-field transport is suppressed. In Ref. 14 it was shown that already a small fraction of these good surfaces or magnetic islands inside the "stochastic sea" can be sufficient to drastically drop the runaway diffusivity, which may easily get even smaller than the thermal transport. In Ref. 10, the transport scaling of Eq. (2) could be experimentally confirmed for standard plasmas; however, "improved confinement" plasmas could be generated where the transport was observed to be independent of the parallel runaway electron velocity, and a reduction in transport from $D \approx 25$ m^2/s to $D \approx 3$ m^2/s was observed. A very interesting observation is reported in Ref. 4. After the injection of a deuterium pellet, an increase in the runaway electron transport up to $D \approx 300$ m^2/s was measured; however, after reaching equilibrium again, the remaining runaways were observed to be narrowly localized and had diffusivities of $D \approx 0.02$ m^2/s, which is a reduction by four orders of magnitude. The explanation that was given is that the pellet injection causes to a complete field stochastization, which is limited in time and leads to large transport described by Eq. (2). However, small island regions would remain, where the fast electrons are not affected. After reaching equilibrium again, these remaining particles dominate the transport.

At this point, it shall be noted that in the present work, we will not attempt to address the second explanation since magnetic islands are beyond its scope. So we concentrate on the possibility of explaining the reduced transport regimes from the assumption of a fully ergodized perturbed magnetic

field. The importance of this approach is twofold. On the one hand, the understanding of the mechanisms of the first explanation will make it easier to decide which mechanism is really responsible for the reduced transport. On the other hand, improvements in the determination of the magnetic field fluctuations are possible since in reality Eq. (2), together with the rather rough orbit correction factor Υ, is frequently used to determine the fluctuation level $\tilde{B}_r/B_0$ out of the diffusivity. This is because the synchrotron radiation of the runaway electrons, their position, and therefore the diffusion coefficient can be measured quite easily, whereas this is not the case for the field fluctuations. So it is possible that corrections may be necessary not concerning the absolute values of the runaway electron transport, but of the magnetic fluctuations.

The remainder of this paper is organized as follows. The conditions under which an orbit averaging approach is valid are reviewed in Sec. II. In Sec. III, we provide some information about the runaway orbit scales and the validity of orbit averaging and gyroaveraging approximations. In Sec. IV, a new approach for the diffusion coefficient, based on perpendicular decorrelation, is presented and compared to the conventional model based on orbit averaging and parallel decorrelation. In Sec. V, a comparison with a number of measurements in literature is made, and a new interpretation of some of the results is suggested. We close with some conclusions in Sec. VI.

II. VALIDITY OF ORBIT AVERAGING

The ordinary orbit averaging procedure as described above assumes that only the magnetic drift velocity is reduced (expressed by the factor Υ or Υ'), but the decorrelation still occurs at $t=\tau_\parallel \sim \pi q R_0/v_\parallel$. This, however, does not need to be true. In the following, we give a short review of the argumentation already presented in Refs. 1 and 2. Figure 2 illustrates the condition that has to be fulfilled for orbit averaging to be valid. The particle has to return into the zone of correlation, which it may temporarily leave due to its perpendicular drift orbit excursion. This is assured for

$$\Xi_{\text{o.a.}} \equiv v_y \frac{T_{\text{orbit}}}{\lambda_\perp} < 1, \tag{6}$$

where v_y is the precession drift, $T_{\text{orbit}}=2\pi q R_0/v_\parallel$ is the orbit circulation time, and $\lambda_\perp$ is the perpendicular correlation length of the magnetic fluctuations. For $\Xi_{\text{o.a.}}>1$, the particle does not return into the correlated zone; therefore, its decorrelation (the transition to diffusive motion) occurs on the smaller time scale

$$\tau^{\text{orbit}} = \frac{T_{\text{orbit}}\lambda_\perp}{2\pi d_r}. \tag{7}$$

Thus, the ansatz leading to Eq. (2) has to be changed, replacing $\tau_\parallel$ by τ^{orbit}, leaving V_B unchanged. We will call this scenario the perpendicular *orbit decorrelation*, in contrast to the ordinary *parallel decorrelation*. As should be clear from Fig. 2, the former scenario is only relevant if $d_r>\lambda_\perp$, which therefore is a second condition in addition to $\Xi_{\text{o.a.}}>1$. A new expression for the diffusion coefficient assuming perpendicular orbit decorrelation is developed in Sec. IV, whereas in Sec. III, the conditions for runaway electrons obeying the different regimes are investigated. For clarification, we would like to mention that the validity of *gyroaveraging*, i.e., the averaging of the fluctuations over one Larmor radius, is not disputed since it occurs on a much smaller time scale, where the deviation due to the precession drift is negligible during one gyroperiod.

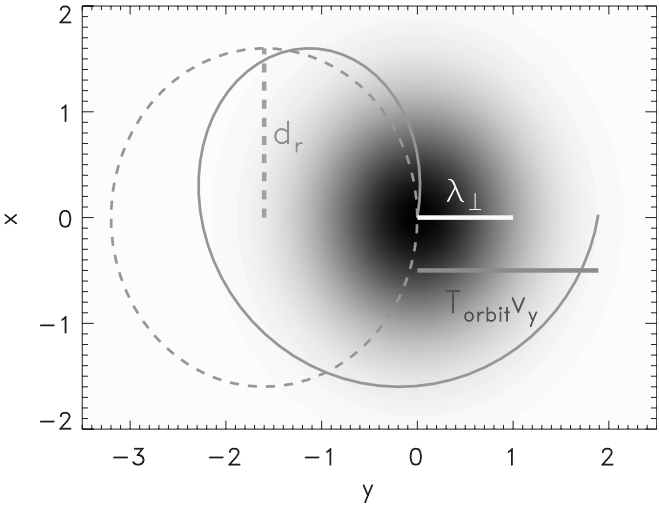

FIG. 2. The dashed line denotes a circle over which the potential is (orbit) averaged for a particle starting at the origin, while the solid line denotes a real particle trajectory with a large precession drift velocity v_y. After one period, the particle is displaced by $T_{\text{orbit}}v_y$ from the origin as well as from the corresponding point on the dashed curve. Therefore, if the particle does not return into the correlated zone [in the background, the autocorrelation function $\langle A_\parallel(0)A_\parallel(\mathbf{x})\rangle$ of an isotropic stochastic magnetic potential with correlation length $\lambda_\perp$ is plotted], orbit averaging is not valid.

III. RUNAWAY ELECTRON ORBITS

In the discussion of fast ion orbits in Refs. 1 and 2, it was not necessary to include relativistic effects since due to the rather large ion mass, they were not relevant for the observed particle energies. For deuterium ions, the classical approach deviates from the relativistic calculation by 10% only at around 260 MeV, whereas this is the case for electrons already at about 70 keV. For energies exceeding 1 MeV, electrons already approach the speed of light.

First, we define the well-known Lorentz factor as

$$\gamma \equiv \frac{1}{\sqrt{1-\frac{v^2}{c^2}}} = \frac{E_{\text{kin}}}{m_0 c^2} + 1, \tag{8}$$

where c is the speed of light. Further, m_0 denotes the rest mass and $m=\gamma m_0$ denotes the relativistic mass. For rewriting the drift orbit parameters of Eq. (1) in Ref. 1 relativistically in terms of the particle's kinetic energy, it is necessary to replace the rest mass by the relativistic mass, and the classical velocity $v=\sqrt{2E/m_0}$ by the relativistic relation $v=c\sqrt{1-1/\gamma^2}$. With these changes, we obtain

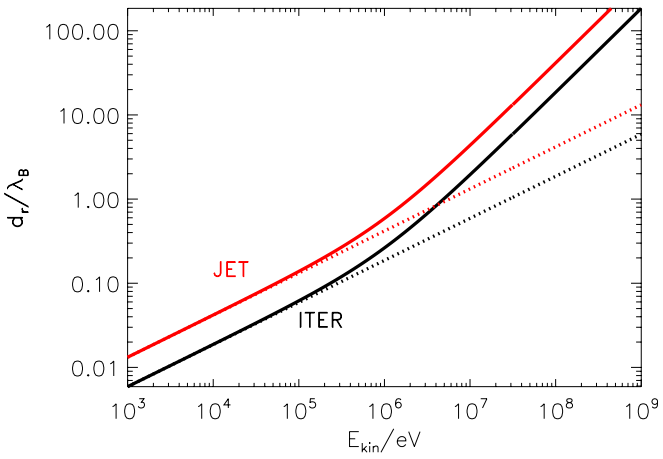

FIG. 3. (Color online) Drift orbit radius normalized to the magnetic fluctuation length vs kinetic energy for runaway electrons with ITER-like (dark/black lines) and JET-like parameters (light/red lines). Solid lines: relativistic calculation according to Eq. (9). Dotted lines: classical limit.

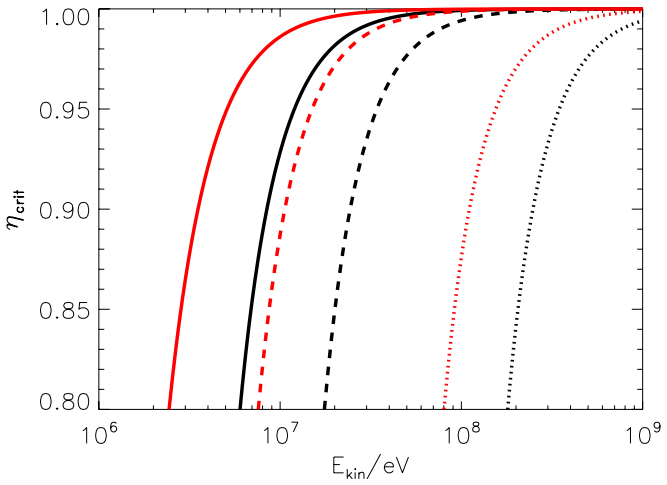

FIG. 4. (Color online) Critical pitch angle η_{crit} vs the electron kinetic energy. $\eta_{crit}(E_{kin})$ is determined as the curve where $\rho_g \equiv a\lambda_B$. Solid lines: $a=0.36$. Dashed lines: $a=1$. Dotted lines: $a=10$. The curves are drawn for ITER-like (dark/black lines) and JET-like parameters (light/red lines). For $\eta > \eta_{crit}$ and $a > 0.36$, the large gyroradius approximation as defined in Eq. (5)—replacing d_r by ρ_g—applies. All curves are calculated relativistically according to Eq. (9). In the classical limit, finite Larmor radius effects would become relevant only for energies exceeding 1 GeV.

$$
\begin{aligned}
T_{\mathrm{orbit}} &= \frac{1}{\sqrt{1-\frac{1}{\gamma^2}}}\frac{2\pi q R_0}{c},\\
d_r &= \sqrt{\gamma^2-1}\frac{q m_0 c}{eB},\\
v_y &= \left(\gamma-\frac{1}{\gamma}\right)\frac{m_0 c^2 \hat{s}}{eBR_0},\\
\rho_g &= \sqrt{\gamma^2-1}\sqrt{1-\eta^2}\frac{m_0 c}{eB}.
\end{aligned}
\tag{9}
$$

Here, T_{orbit} is the drift orbit circulation time, d_r is the orbit radius (half of the maximum deviation from the particle's initial flux surface), v_y denotes the toroidal precession drift, and ρ_g is the gyroradius. The pitch angle is defined as $\eta \equiv v_\parallel / v$. Since runaway electrons have a pitch angle close to 1 (in Refs. 8 and 15, $\eta=0.98$ was found), the parameter η is neglected in the first three expressions.

For the turbulence parameters, we chose $\hat{\lambda}_B=2.5\rho_s$ (perpendicular magnetic correlation length), $\hat{\lambda}_c=6\rho_s$ (perpendicular electrostatic correlation length), and $\hat{V}_E=3c_s\rho_s/R_0$ (mean $E\times B$ drift velocity), as was found by GENE simulations,[1,2] where c_s denotes the ion sound speed and ρ_s denotes the respective gyroradius. Further, we set $\tilde{B}_r/B_0=10^{-4}$ for the plots presented here similar to the value found in Ref. 1. We will apply orbit approaches for typical parameters of different fusion devices. For ITER parameters, we take $R_0=6.2$ m, $B_0=5.3$ T, and $T_e=10$ keV, whereas for JET parameters, we take $R_0=3.0$ m, $B_0=2.75$ T, and $T_e=2$ keV. For curves based on TEXTOR data, we apply the parameters $R_0=1.75$ m, $B_0=2.25$ T, and $T_e=2$ keV. Further, we chose $q=2$, $\hat{s}=0.8$ for all three cases. It shall be emphasized that while these values may be viewed as typical, they should not be regarded as fixed. The JET parameters are chosen so to compare our scaling approach to the results published in Ref. 7, where the orbit averaging approach[9] was used. Since larger machine sizes go along with larger fields and temperatures, we will find that the absolute values of the orbits and diffusivities do not differ too much.

Figure 3 shows the drift orbit radius d_r normalized to the magnetic field correlation length for both the ITER and the JET parameters. Between 2 and 5 MeV, the orbit radius exceeds the correlation length, which means that either orbit averaging effects [as described by Eq. (4) or Eq. (5)] or orbit decorrelation [as described later by Eq. (10)] occur. As can also be observed, relativistic effects are responsible for a stronger increase in d_r for large energies.

Further, we want to include the influence of finite gyroradius effects. In the discussion in Ref. 13, we have claimed that they become relevant for $\rho_g/\lambda_B \gtrsim 0.36$. In contrast to the orbit radius, the gyroradius has a sensitive pitch angle dependence for large pitch angles since it is proportional to $\sqrt{1-\eta^2}$. Therefore, in Fig. 4 the critical pitch angle (where $\rho_g/\lambda_B=0.36$) is plotted versus the electron energy. Only for pitch angles exceeding η_{crit} that finite gyroradius effects can be ignored. We see that for $\eta=0.98$ (as measured in Refs. 8 and 15), they become relevant for energies larger than 10–20 MeV; however, they get stronger influence only for higher energies when the gyroradius clearly exceeds the correlation length.

We have already addressed the question whether the orbit averaging approach, on which the determinations of Υ in Eqs. (4) and (5) are based, is valid or not for highly energetic runaway electrons. In Sec. II, this question has already been discussed (based on Refs. 1 and 2), introducing an *orbit averaging validity parameter* $\Xi_{\mathrm{o.a.}}=v_y T_{\mathrm{orbit}}/\lambda_\perp$. For $\Xi_{\mathrm{o.a.}} \lesssim 1$, the orbit averaging approach is valid, whereas for $\Xi_{\mathrm{o.a.}} \gtrsim 1$, it is not since decorrelation occurs on a time scale smaller than

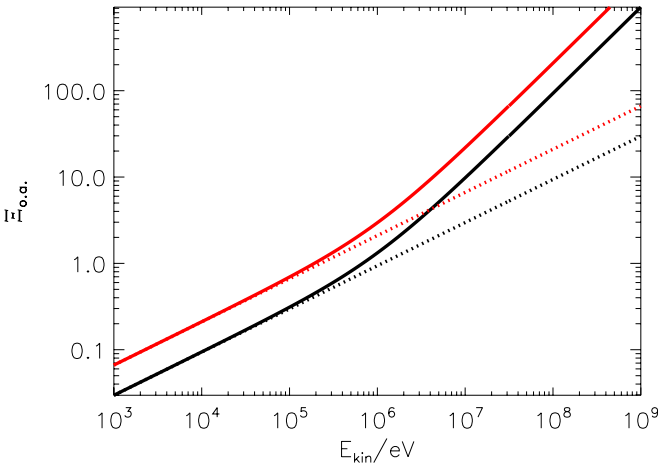

FIG. 5. (Color online) Orbit averaging validity parameter $\Xi_{\text{o.a.}}$ vs kinetic energy for runaway electrons with ITER-like (dark/black lines) and JET-like parameters (light/red lines). Solid lines: relativistic calculation according to Eq. (9). Dotted lines: classical limit.

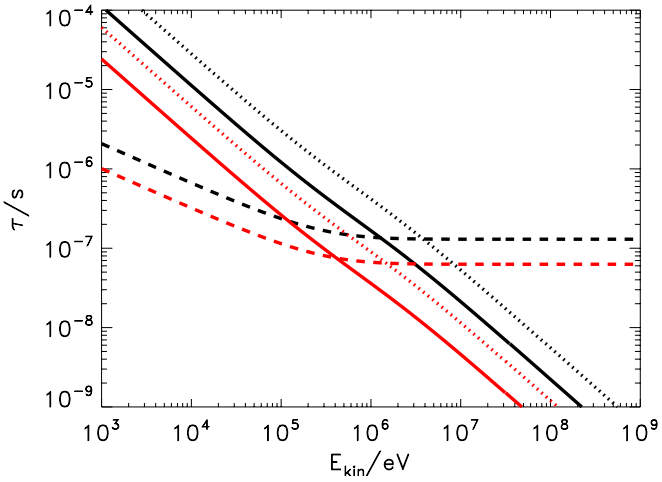

FIG. 6. (Color online) Relevant time scales for the particle diffusivity vs kinetic energy. Solid lines: orbit decorrelation time $\tau^{\text{orbit}} \equiv \lambda_B T_{\text{orbit}}/2\pi d_r$. Dashed lines: parallel decorrelation time $\tau_\parallel \equiv \lambda_\parallel / v_\parallel \sim \pi q R_0 / v_\parallel$. Dotted lines: drop time $\tau_{\text{drop}} \equiv 2\lambda_B / v_y$. The curves are drawn for ITER-like (dark/black lines) and JET-like parameters (light/red lines) and calculated relativistically according to Eq. (9).

the orbit circulation time by the particle motion perpendicular to the magnetic field.

In Fig. 5, $\Xi_{\text{o.a.}}$ is plotted versus the particle energy. We note that for $E_{\text{kin}} > 10$ keV, v_y is the dominating velocity for the perpendicular particle motion. As can be observed, $\Xi_{\text{o.a.}} > 1$ for E_{kin} exceeding 200–700 keV, which means that typical runaway electrons are clearly not in an orbit averaging regime, wherefore the approaches of Eqs. (4) and (5) are not valid.

Before calculating diffusion coefficients, we have to recall some features of the decorrelation process responsible for the transition to a diffusive behavior. As pointed out in Ref. 2, it is of special importance which of the times $\tau_\parallel$, τ^{orbit}, and τ_{drop} is the smallest one. Here, as defined before, $\tau_\parallel$ is the parallel decorrelation time, and $\tau^{\text{orbit}} \equiv T_{\text{orbit}} \lambda_B / (2\pi d_r)$ is the perpendicular decorrelation time, i.e., the time a particle needs to decorrelate due to its orbit shift perpendicular to the magnetic field lines (this is, of course, relevant only if $d_r \gtrsim \lambda_B$). The smaller of these two time scales is responsible for the transition into the diffusive regime. $\tau_{\text{drop}} \equiv 2\lambda_B / v_y$ is the so-called "drop time,"[16] which defines the scale of a sharp drop in the diffusion coefficient, caused by a "drift barrier" built up by the toroidal precession drift. It is relevant only if it is smaller than the decorrelation time.

As can be inferred from Fig. 6, τ_{drop} is always larger than the minimum of orbit decorrelation time τ^{orbit} and parallel decorrelation time $\tau_\parallel$. This means that the drift barrier due to the toroidal precession drift (as described in Ref. 16) has no influence since decorrelation always occurs on a smaller time scale. For energies smaller than about 500 keV–1 MeV, the parallel motion provides the relevant decorrelation mechanism, whereas for larger energies, decorrelation occurs due to the perpendicular orbit motion, as already described in Refs. 1 and 2.

So we can state the following.

(1) For the perpendicular orbit decorrelation scaling to be valid, the following assumptions have to be fulfilled: $\Xi_{\text{o.a.}} > 1$, $d_r > \lambda_B$, $\tau^{\text{orbit}} < \tau_\parallel$. So according to Figs. 3, 5, and 6, it is the orbit diameter which is the limiting value, leading to the precondition that $E_{\text{kin}} \gtrsim$ "some MeV." For larger values ($E_{\text{kin}} \gtrsim 10$ MeV for $\eta \approx 0.98$), finite gyroradius effects have to be taken into account additionally.

(2) On the contrary, for the particles following the perturbed magnetic field lines, only $\Xi_{\text{o.a.}} < 1$ has to be fulfilled, i.e., $E_{\text{kin}} \lesssim$ "some hundreds of keV." In that case, the parallel motion leads to decorrelation at $\tau_\parallel$ and to the saturation of the diffusion coefficient so that the approach of Eqs. (2) and (3), together with Eq. (5), is valid. In the range between these extremes, orbit averaging is not valid; however, the orbit diameter is still too small for perpendicular orbit decorrelation to occur. We will not examine this transition regime more closely here, but assume a continuous transfer from regime 2 to regime 1.

IV. DIFFUSION COEFFICIENT ASSUMING ORBIT DECORRELATION

The diffusion coefficient for case 2 has already been described. Now, we want to establish relations for case 1, i.e., the orbit decorrelation mechanism already introduced briefly in Sec. II. Using the orbit parameters of Eq. (9), we obtain

$$D_M \approx \frac{2}{3} V_B^2 \tau^{\text{orbit}} = \frac{2}{3} \left(\frac{\tilde{B}_r}{B_0} \right)^2 v_\parallel^2 \frac{\lambda_B T_{\text{orbit}}}{2\pi d_r}$$

$$= \frac{2}{3} \left(\frac{\tilde{B}_r}{B_0} \right)^2 \frac{\lambda_B R_0 e B}{m_0} \frac{1}{\gamma} \equiv \pi q R_0 V_B^2 / v_\parallel \Upsilon''. \quad (10)$$

Similarly, for electrostatic transport, we find

$$D_E \approx \frac{2}{3} V_E^2 \tau^{\text{orbit}} = \frac{2}{3} \frac{V_E^2 \lambda_V R_0 eB}{m_0 c^2} \frac{1}{\gamma - 1/\gamma} \equiv \pi q R_0 V_E^2 / v_\parallel \Upsilon''. \tag{11}$$

In order to express these equations analogous to Eqs. (2) and (3), a new finite orbit correction factor Υ'' has been implicitly defined, which can be calculated as

$$\Upsilon'' = \lambda_B / \left(\tfrac{3}{2} \pi d_r\right). \tag{12}$$

This factor is slightly larger than the orbit averaging approach of Eq. (5) for $d_r \gtrsim \lambda_B$, based on Ref. 13, but clearly smaller (by a factor of 4.7) than the assumption expressed by Eq. (4), based on Ref. 9.

We recall that the perpendicular orbit decorrelation approach (Υ'') is valid only in the range $E_{\text{kin}} \gtrsim 1$ MeV, whereas below that, the field line diffusion approach, modified by Υ', is valid. Interestingly, the factor Υ''—derived using the model of perpendicular orbit decorrelation—corresponds to the factor Υ'—derived using the (invalid) orbit averaging approach—quite well, except for a small difference in the prefactor. Is this a systematic effect or pure chance? The dependence of Υ' (or Υ) on λ_B / d_r comes from the reduction in the average magnetic drift velocity due to orbit averaging, whereas in the orbit decorrelation case, the scaling of Υ'' is governed by the reduction in the effective decorrelation time. So, it is reasonable to attribute the similarity to an accidental coincidence. If the effective Kubo number was larger than 1, the two approaches would differ from each other again. However, as could be confirmed by numerical simulations in Ref. 2, the perpendicular orbit decorrelation approach reproduces the correct diffusivities best.

Moreover, as could be demonstrated in Ref. 2, it is especially the strong influence of the toroidal precession drift, forming a potential barrier in the system comoving with the particle, which is responsible for the strong reduction of diffusivity in the case that orbit averaging is valid. In Fig. 6, it can be seen that for large runaway particle energies, $\tau_{\text{drop}} < \tau_\parallel$, which means that if the (faster) perpendicular decorrelation mechanism was ignored, the drift barrier would dominate the transport, leading to a much steeper decrease in D with E than expressed by the factor Υ' in Eq. (5) [or Υ in Eq. (4)]. Using the perpendicular orbit decorrelation approach, however, the drift barrier has no influence since $\tau^{\text{orbit}} < \tau_{\text{drop}}$. Therefore, we can state that the coincidence of the orbit averaging approach and the orbit decorrelation mechanism is not only accidental in the sense that different approaches lead to the same scaling law, it is also only possible since in the former case the effect of the drift barrier is completely ignored, and a combination of two wrong assumptions (orbit averaging and omission of the drift barrier) leads to almost the correct result by chance. Nevertheless, since the transition to the diffusive regime occurs on different time scales in both approaches, situations may occur where it becomes important to be aware of the real mechanisms at work.

In Fig. 7, the field line diffusion according to Eq. (2) [including orbit averaging corrections for $d_r \lesssim \lambda_B$, Eq. (5)] for small kinetic energies is combined with the orbit decorrelation for large kinetic energies according to Eq. (10) to a continuous curve, which gives something like the expected real behavior of runaway magnetic diffusivity. The solid curves neglect finite gyroradius effects, whereas the dashed curves include them for an assumed pitch angle of $\eta = 0.98$, as found in Refs. 8 and 15. For small energies, the particles behave nonrelativistically and essentially follow the magnetic field lines, and the diffusivity simply increases with $v_\parallel \propto \sqrt{E}$. For energies exceeding 100 keV, relativistic effects as well as orbit averaging effects start to reduce the increase and eventually reverse it. For larger energies, the perpendicular orbit decorrelation scaling according to Eq. (10) applies. Since $v_\parallel$ and T_{orbit} saturate due to the relativistic increase in mass, but the orbit radius shows an increase proportional to the kinetic energy [see Eq. (9)], the diffusion coefficient declines as E^{-1} in the case that finite Larmor radius effects are negligible. Including them leads to an additional factor E^{-1}, which results in an overall scaling of $D_M(E) \propto E^{-2}$. Depending on the pitch angle, this last transition can occur at larger or smaller energies. Once more, it shall be emphasized that the difference between the scaling laws illustrated in Fig. 7 and the ones presented in Ref. 1 lies only in the relativistic behavior of the runaway electrons. Since the gyroradius and orbit radius grow stronger with energy than in the classical limit, but the orbit circulation time is limited due to the upper limit for the particle's velocity, the decline in diffusivity according to Eq. (10) is much stronger.

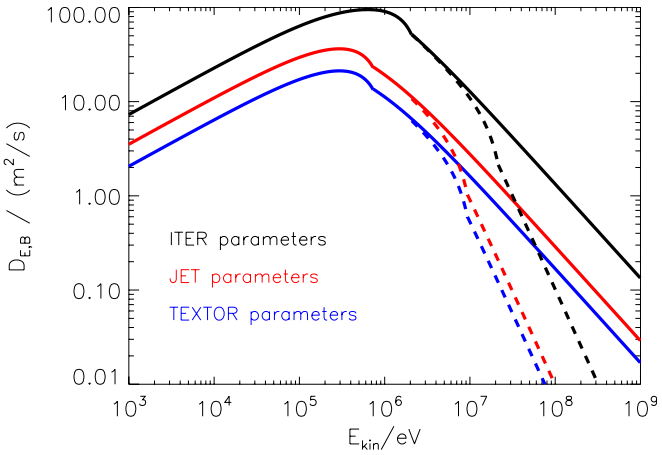

FIG. 7. (Color online) Magnetic diffusion coefficients vs kinetic energy. Combined approach taking the field line diffusion model with orbit averaging [Eq. (2)] for small energies ($\Xi_{\text{o.a.}} < 1$, $d_r < \lambda_B$) and the orbit decorrelation model [Eq. (10)] for large energies ($\Xi_{\text{o.a.}} > 1$, $d_r > \lambda_B$) As before, $\tilde{B}_r / B_0 = 10^{-4}$ was chosen. Solid curves: no finite gyroradius effects ($\eta \to 1$). Dashed lines: finite gyroradius effects included for $\eta = 0.98$ using gyroaveraging. The curves are drawn for ITER-like (black/upper lines), JET-like (red/middle lines), and TEXTOR-like parameters (blue/lower lines) and calculated relativistically according to Eq. (9).

V. COMPARISON WITH LITERATURE

We now want to compare the consequences of our results with those of previous publications, paying special attention to the determination of $\tilde{B}_r / B_0$. At the JET tokamak,[7] the diffusion coefficient of runaway electrons was measured

in the energy range between 133 keV and about 1.5 MeV using a fast electron bremsstrahlung diagnostic. A diffusion coefficient averaged over that energy range was determined to be $D=0.2$ m^2/s. Since finite orbit effects are negligible for the smallest energy which was measured, $E_{\mathrm{kin}}=133$ keV, the magnetic field fluctuations were determined according to Eq. (2) to be $\tilde{B}_r/B_0 \approx 8\times10^{-6}$. However, this value was regarded as a lower limit since it was claimed that for larger energies, the finite orbit influence would increase; therefore, the magnetic field perturbation should increase to obtain the measured value of D. The solid red curve in Fig. 7 describes the realistic diffusion coefficient for arbitrary energies neglecting finite gyroradius effects and has been normalized exactly to the values of Ref. 7, except that $\tilde{B}_r/B_0=10^{-4}$ was taken. If we replace that value by $\tilde{B}_r/B_0 \approx 8\times10^{-6}$ in Eq. (2), this would lead to a reduction in the $D(E)$ curves by a factor of 156, which would give a maximum value of exactly $D=0.2$ m^2/s. However, it was pointed out in Ref. 7 that the maximum runaway electron energy is about 30 MeV. Here, according to Fig. 7, the diffusion coefficient should be expected to be smaller than the value around 300 keV by a factor of about 30 (without finite gyroradius effects), i.e., $D\approx0.007$ m^2/s. Assuming $\eta=0.98$, we would even find $D\approx0.0009$ m^2/s. Unfortunately, diffusivities were not measured in the high energy limit in Ref. 7.

At the TEXTOR tokamak, different diffusion regimes were found, which were explained by a different level of stochastization of the magnetic field lines.[4] By synchrotron emission, a population of 30 MeV runaway electrons was observed. After pellet injection, a rapid loss has been detected with diffusion coefficients up to 300 m^2/s. If we apply Eq. (10) (or adjust Fig. 7), we find the corresponding magnetic field perturbation to be $\tilde{B}_r/B_0=2.3\times10^{-3}$ if finite gyroradius effects are neglected, which is a rather large value. However, according to the relation $\tilde{B}_r/B_0 \sim C(\beta/\beta_{\mathrm{crit}})\rho_s/R_0$,[1] we can approximate the maximal possible value to $(\tilde{B}_r/B_0)_{\max}\sim\rho_i/R_0\approx2.9\times10^{-3}$, which means that such a large value can, in principle, be possible. Since the pellet injection raises the plasma pressure and therefore also the plasma beta, such a behavior can be qualitatively understood. Including the effects of a finite gyroradius with the assumption $\eta=0.98$, we would obtain $(\tilde{B}_r/B_0)_{\max}\approx7\times10^{-3}$, a value which would actually be too large. However, it must be emphasized that the real pitch angle is unknown in that experiment. Moreover, in Ref. 4 it is assumed that all runaway electrons have 30 MeV, which need not be true. If a significant number of lower energetic electrons exist, their diffusivity can reach the measured value for smaller values of $(\tilde{B}_r/B_0)$. Now after pellet injection, a remaining runaway electron population with an extremely slow diffusivity of $D\lesssim0.02$ m^2/s was detected, which was attributed to the existence of intact magnetic islands within the chaotic sea. However, if we assume stochasticity also here and apply the standard orbit decorrelation approach without gyroradius effects, this corresponds to $\tilde{B}_r/B_0\approx1.9\times10^{-5}$, which is still a reasonably large number. Assuming again $\eta=0.98$ and including the finite gyroradius effects resulting from this choice, we would even obtain $\tilde{B}_r/B_0\approx1.7\times10^{-4}$, which would be an ordinary magnitude. The diffusion coefficients derived that way correspond to findings reported from TEXTOR,[6] where $\tilde{B}_r/B_0\approx5\times10^{-5}$ was found for Ohmic plasmas, but $\tilde{B}_r/B_0\approx10^{-3}$ if a NBI current is applied. Similar findings are reported from the Tore Supra tokamak.[17] Here, the determination of the magnetic field fluctuations was done directly via the polarization change in electromagnetic waves scattered by the fluctuations, thus independent of a determination of the diffusion coefficient. So it may possibly be that the concept of good surfaces and magnetic islands is not necessary for understanding the observed small diffusion coefficients since they can also be explained conventionally by our model, assuming stochastic field fluctuations of the order of 10^{-5}–10^{-4}, as reported in literature. However, an exact determination of $\tilde{B}_r/B_0$ strongly depends on the knowledge of the pitch angle, which is normally not known from measurements. In literature reviewed here, finite gyroradius effects have always been neglected, which indicates that, in general, the determination of the field fluctuations has led to values that are too small.

VI. SUMMARY AND CONCLUSIONS

We have applied the same mechanisms to fast runaway electrons that were previously applied to fast ions. As before, orbit averaging was found to be invalid for large particle energies so that the orbit decorrelation mechanism has to be used to describe transport correctly. Due to their smaller mass and higher energy, runaway electrons behave strongly relativistically, which leads to different scaling laws compared to nonrelativistic ions. For example, the magnetic transport drops with $1/E$ for large energies as long as the pitch angle is large enough for finite gyroradius effects to be negligible. If this is no longer the case, we obtain even $D\propto E^{-2}$. It was found that despite the wrong ansatz, orbit averaging leads to a similar result in the case that the influence of the toroidal precession drift is neglected. While the transport is found to be weak for runaway electrons close to saturation, a maximum is found around 1 MeV, which may strongly exceed the thermal transport. Due to the quadratic dependence, the magnetic field perturbation was shown to be a crucial parameter. Perturbations as measured in experiments are found to be, in principle, sufficient to explain the weak transport for large kinetic energies if the perpendicular orbit decorrelation approach is used together with finite gyroradius effects. However, they strongly depend on the pitch angle, which is a quantity often unknown, so that the determination of $\tilde{B}_r/B_0$ is afflicted with some uncertainties.

[1] T. Hauff, M. J. Pueschel, T. Dannert, and F. Jenko, Phys. Rev. Lett. **102**, 075004 (2009).
[2] T. Hauff and F. Jenko, Phys. Plasmas **15**, 112307 (2008).
[3] J. Wesson, *Tokamaks* (Clarendon, Oxford, 1987), Chap. 3.
[4] R. Jaspers, N. J. Lopes Cardozo, K. H. Finken, B. C. Schokker, G. Mank, G. Fuchs, and F. C. Schuller, Phys. Rev. Lett. **72**, 4093 (1994).
[5] I. Entrop, N. J. Lopez Cardozo, R. Jaspers, and K. H. Finken, Plasma Phys. Controlled Fusion **40**, 1513 (1998).
[6] I. Entrop, N. J. Lopez Cardozo, R. Jaspers, and K. H. Finken, Phys. Rev. Lett. **84**, 3606 (2000).

[7]B. Esposito, R. M. Solis, and P. van Belle, Plasma Phys. Controlled Fusion **38**, 2035 (1996).
[8]R. Jaspers, N. J. Lopes Cardozo, F. C. Schuller, K. H. Finken, T. Grewe, and G. Mank, Nucl. Fusion **36**, 367 (1996).
[9]J. R. Myra and P. J. Catto, Phys. Fluids B **4**, 176 (1992).
[10]R. O'Connell, D. J. Den Hartog, C. B. Forest, J. K. Anderson, T. M. Biewer, B. E. Chapman, D. Craig, G. Fiksel, S. C. Prager, J. S. Sarff, and S. D. Terry, Phys. Rev. Lett. **91**, 045002 (2003).
[11]P. Helander, L.-G. Eriksson, and F. Andersson, Plasma Phys. Controlled Fusion **44**, B247 (2002).
[12]A. Wingen, S. S. Abdullaev, K. H. Finken, M. Jakubowski, and K. H. Spatschek, Nucl. Fusion **46**, 941 (2006).
[13]T. Hauff and F. Jenko, Phys. Plasmas **13**, 102309 (2006).
[14]C. C. Hegna and J. D. Callen, Phys. Fluids B **5**, 1804 (1993).
[15]Z. Y. Chen, B. N. Wan, S. Y. Lin, Y. J. Shi, and L. Q. Hu, Phys. Lett. A **351**, 413 (2006).
[16]T. Hauff and F. Jenko, Phys. Plasmas **14**, 092301 (2007).
[17]X. L. Zou, L. Colas, M. Paume, J. M. Chareau, L. Laurent, P. Devynck, and D. Gresillon, Phys. Rev. Lett. **75**, 1090 (1995).